

# Red clump stars of the Milky Way – laboratories of extra-mixing

G. Tautvaišienė,<sup>1\*</sup> G. Barisevičius,<sup>1</sup> Y. Chorniy,<sup>1</sup> I. Ilyin,<sup>2</sup> and E. Puzeras<sup>1</sup>

<sup>1</sup>*Institute of Theoretical Physics and Astronomy, Vilnius University, Goštauto 12, Vilnius 01108, Lithuania*

<sup>2</sup>*Leibniz Institut für Astrophysik Potsdam, An der Sternwarte 16, Potsdam 14482, Germany*

Accepted 2012 December 18. Received 2012 December 18; in original form 2012 November 26

## ABSTRACT

In this work we present the main atmospheric parameters, carbon, nitrogen and oxygen abundances, and  $^{12}\text{C}/^{13}\text{C}$  ratios determined in a sample of 28 Galactic clump stars. Abundances of carbon were studied using the  $\text{C}_2$  band at 5086.2 Å. The wavelength interval 7980–8130 Å with strong CN features was analysed in order to determine nitrogen abundances and  $^{12}\text{C}/^{13}\text{C}$  isotope ratios. The oxygen abundances were determined from the [O I] line at 6300 Å. The mean abundances of C, N and O abundances in the investigated clump stars support our previous estimations that, compared to the Sun and dwarf stars of the Galactic disk, carbon is depleted by about 0.2 dex, nitrogen is enhanced by 0.2 dex and oxygen is close to abundances in dwarfs. The  $^{12}\text{C}/^{13}\text{C}$  and C/N ratios for galactic red clump stars analysed were compared to the evolutionary models of extra-mixing. The steeper drop of  $^{12}\text{C}/^{13}\text{C}$  ratio in the model of thermohaline mixing by Charbonnel & Lagarde better reflects the observational data at low stellar masses than the more shallow model of cool bottom processing by Boothroyd & Sackman. For stars of about  $2 M_{\odot}$  masses a modelling of rotationally induced mixing should be considered with rotation of about  $250 \text{ km s}^{-1}$  at the time when a star was at the hydrogen-core-burning stage.

**Key words:** stars: abundances – stars: evolution – stars: horizontal-branch.

## 1 INTRODUCTION

Investigations of galactic red clump stars may help to find fundamental answers to questions concerning mechanisms of transport of processed material to the stellar surface in low mass stars. Post-main-sequence stars with masses below  $2 - 2.5 M_{\odot}$  exhibit signatures of material mixing that require challenging modelling beyond the standard stellar theory. Carbon and nitrogen abundances are among most useful quantitative indicators of mixing processes in evolved stars. Already Iben (1965) has evaluated that the first dredge-up lowers abundances of  $^{12}\text{C}$  by about 30 per cent and abundances of  $^{14}\text{N}$  increase by about 80 per cent. Later on it was noticed that atmospheric abundances of stars are affected not only by the first dredge-up, but also by extra-mixing (Day, Lambert & Sneden 1973; Pagel 1974; Tomkin, Luck & Lambert 1976; Lambert & Ries 1981; Gilroy 1989; Gilroy & Brown 1991; Tautvaišienė et al. 2000, 2001, 2005; Mikolaitis et al. 2010, 2011a,b, 2012, and references therein).

The extra-mixing becomes efficient at once after the luminosity function bump of the giant branch, i.e. the evolu-

tionary point where the hydrogen-burning shell crosses the chemical discontinuity created by the outward moving convective envelope (Charbonnel 1994; Charbonnel, Brown & Wallerstein 1998). The alterations depend on stellar mass, metallicity and evolutionary stage (e.g. Lambert & Ries 1977; Boothroyd & Sackmann 1999; Gratton et al. 2000, Spite et al. 2006; Charbonnel & Zahn 2007; Recio-Blanco & de Laverny 2007; Tautvaišienė et al. 2007, 2010; Smiljanic et al. 2009).

Nowadays various mechanisms of extra-mixing were proposed by a number of scientific groups (see reviews by Chanamé, Pinsonneault & Terndrup 2005; Charbonnel 2006; and recent papers by Cantiello & Langer 2010; Denissenkov 2010; Lagarde et al. 2011; Palmerini et al. 2011; Wachlin, Miller Bertolami & Althaus 2011; Angelou et al. 2012).

The  $^{12}\text{C}/^{13}\text{C}$  ratio is the most robust diagnostic of deep mixing, because it is very sensitive to mixing processes and is almost insensitive to the adopted stellar parameters. We aim to study abundances of carbon isotopes, nitrogen and oxygen in an accurate and homogeneous way for a significant sample of clump star of the Galaxy.

The *Hipparcos* catalogue (Perryman et al. 1997) contains about 600 clump stars with parallax errors lower than

\* E-mail: grazina.tautvaisiene@tfai.vu.lt

10 per cent and represents a complete sample of clump stars to a distance of about 125 pc. Almost a half of these stars are already investigated by means of high resolution spectroscopy (Tautvaišienė et al. 2003; Mishenina et al. 2006; Liu et al. 2007; Luck & Heiter 2007; Tautvaišienė & Puzeras 2009; Puzeras et al. 2010); however, for the determination of carbon isotope ratios so far only our Paper I (Tautvaišienė et al. 2010) was dedicated.

In Paper I, we have determined  $^{12}\text{C}$ ,  $^{13}\text{C}$ , N and O abundances in atmospheres of 34 Galactic red clump stars. In this study the same data are determined for other 28 stars. The results of  $^{12}\text{C}/^{13}\text{C}$  and C/N ratios obtained in Paper I and this work for the clump stars are compared with the available theoretical models of extra-mixing.

As concerns the red clump of our Galaxy, it was always interesting to find out what fraction of stars in the Galactic clump are first ascent giants and how many of them are He-core-burning stars (e.g. Mishenina et al. 2006; Paper I). As it was shown in Paper I, carbon isotope ratios allow us to obtain this information as well.

## 2 OBSERVATIONAL DATA AND METHOD OF ANALYSIS

Spectra were obtained at the Nordic Optical Telescope (NOT, La Palma) in 2006 December with the SOFIN échelle spectrograph (Tuominen, Ilyin & Petrov 1999). The second optical camera ( $R \approx 80\,000$ ) was used to observe simultaneously 13 spectral orders, each of 40–60 Å in length, located from 5650 Å to 8130 Å. Two observations have been carried out for every star. A CCD frame was centered on carbon and nitrogen features during the first observation, and during the second on the forbidden oxygen line. The reduction of CCD images was done using the 4A software package (Ilyin 2000). Procedures of bias subtraction, cosmic ray removal, flat field correction, scattered light subtraction, and extraction of spectral orders were used for image processing. A Th-Ar comparison spectrum was used for the wavelength calibration. The continuum was defined from a number of narrow spectral regions, selected to be free of lines.

The spectra were analysed using a differential model atmosphere technique. The EQWIDTH and BSYN program packages, developed at the Uppsala Astronomical Observatory, were used to carry out the calculation of abundances from measured equivalent widths and synthetic spectra, respectively. A set of plane parallel, line-blanketed, constant-flux LTE model atmospheres was computed with an updated version of the MARCS code (Gustafsson et al. 2008).

Effective temperature, gravity and microturbulence were derived using traditional spectroscopic criteria. The preliminary effective temperatures for the stars were determined using the  $(B-V)_o$  and  $(b-y)_o$  colour indices and the temperature calibrations by Alonso, Arribas & Martínez-Roger (1999). All the effective temperatures were carefully checked and corrected, if needed, by forcing Fe I lines to yield no dependency of iron abundance on excitation potential by changing the model effective temperature. Surface gravity was obtained by forcing Fe I and Fe II lines to yield

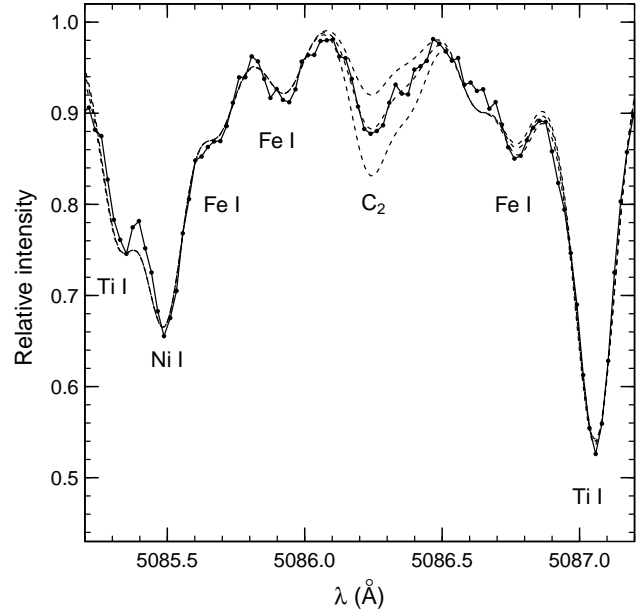


**Figure 1.** Synthetic and observed spectra for the  $\text{C}_2$  region around  $\lambda 5086$  Å of HD 417. The solid line shows the observed spectrum and the dashed lines show the synthetic spectra generated with  $[\text{C}/\text{Fe}] = -0.33, -0.23$  and  $-0.13$ .

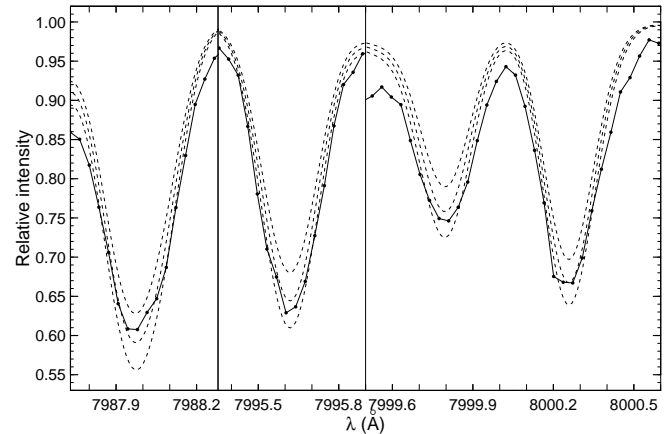


**Figure 2.** Stellar spectrum synthesis example around CN lines in HD 6. The solid line shows the observed spectrum and the dashed lines show the synthetic spectra generated with  $[\text{N}/\text{Fe}] = 0.12, 0.22$  and  $0.32$ .

the same  $[\text{Fe}/\text{H}]^1$  value by adjusting the model gravity. The microturbulence value corresponding to minimal line-to-line Fe I abundance scattering was chosen as the correct value. Equivalent widths of 25–27 Fe I and 9–12 Fe II lines were used for the determination of atmospheric parameters. The equivalent widths of the lines were measured by fitting a Gaussian profile using the 4A software package (Ilyin 2000). Using the  $gf$  values and solar equivalent widths of analysed iron lines from Gurtovenko & Kostik (1989), we obtained the solar iron abundance, later used for the differential determination of iron abundances in the programme stars. We

<sup>1</sup> In this paper we use the customary spectroscopic notation  $[\text{X}/\text{Y}] \equiv \log_{10}(N_{\text{X}}/N_{\text{Y}})_{\text{star}} - \log_{10}(N_{\text{X}}/N_{\text{Y}})_{\odot}$

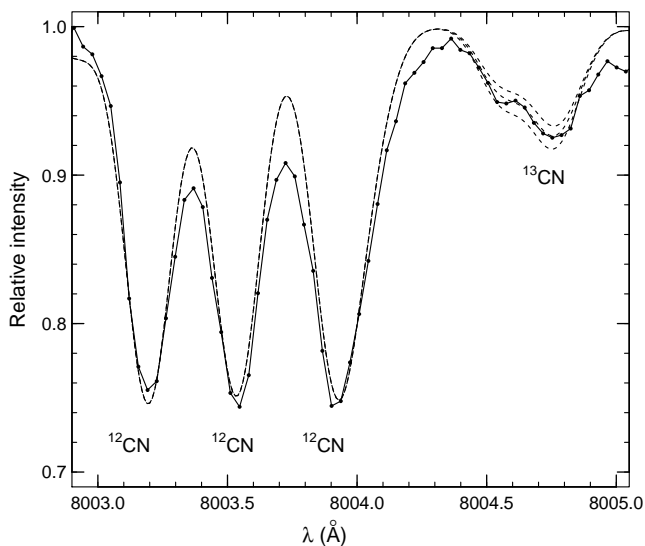


**Figure 3.** Stellar spectrum synthesis example around CN lines in the first ascent giant HD 6. The solid line shows the observed spectrum and the dashed lines show the synthetic spectra generated with  $^{12}\text{C}/^{13}\text{C}$  equal to 22 (upper line), 19 (middle line), and 16 (lower line).

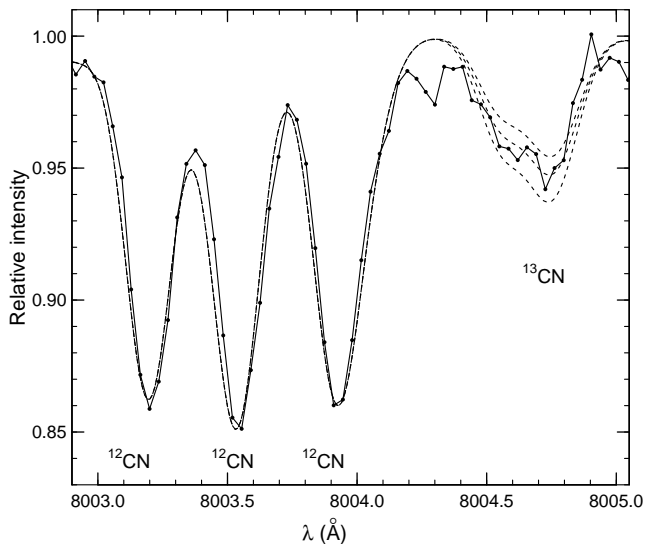


**Figure 4.** Stellar spectrum synthesis example around CN lines in the helium-core-burning star HD 55730. The solid line shows the observed spectrum and the dashed lines show the synthetic spectra generated with  $^{12}\text{C}/^{13}\text{C}$  equal to 12 (upper line), 10 (middle line), and 8 (lower line).

used the solar model atmosphere from the set calculated in Uppsala with a microturbulent velocity of  $0.8 \text{ km s}^{-1}$ , as derived from Fe I lines.

Carbon abundances were determined in stars using the  $5085 - 5087 \text{ \AA}$  interval with the  $\text{C}_2$  band at  $5086.2 \text{ \AA}$ . The band at  $5635.5 \text{ \AA}$ , which we used in Paper I, this time appeared at the very edge or outside the CCD frame, so following studies by Lambert & Ries (1981) and Gratton et al. (2006) we have decided to analyse  $\text{C}_2 \lambda 5086.2 \text{ \AA}$ . We have checked the carbon abundance results given by both bands on HD 225216 and were satisfied by the agreement. The in-

terval  $7980 - 8130 \text{ \AA}$  contains strong  $^{12}\text{C}^{14}\text{N}$  and  $^{13}\text{C}^{14}\text{N}$  features, so it was used for the nitrogen abundance and  $^{12}\text{C}/^{13}\text{C}$  ratio analysis. The well known  $^{13}\text{CN}$  line at  $8004.7 \text{ \AA}$  was analysed in order to determine  $^{12}\text{C}/^{13}\text{C}$  ratios. The molecular data for  $\text{C}_2$  and CN bands were provided by colleagues from the Uppsala Astronomical Observatory and slightly adjusted to fit the solar spectrum (Kurucz 2005) with the solar abundances by Grevesse & Sauval (2000). We present several examples of spectral syntheses of  $\text{C}_2$  and CN features and comparisons to the observed spectra in Figs. 1 – 4.

We derived oxygen abundances from the synthesis of the forbidden [O I] line at  $6300 \text{ \AA}$  (Fig. 5 and 6). The  $gf$  values for  $^{58}\text{Ni}$  and  $^{60}\text{Ni}$  isotopic line components, which blend the oxygen line, were taken from Johansson et al. (2003) and [O I]  $\log gf = -9.917$  value, as calibrated to the solar spectrum (Kurucz 2005).

The atomic oscillator strengths for stronger lines of iron and other elements were taken from Gurtovenko & Kostik (1989). The Vienna Atomic Line Data Base (VALD, Piskunov et al. 1995) was extensively used in preparing the input data for the calculations. In addition to thermal and microturbulent Doppler broadening of lines, atomic line broadening by radiation damping and van der Waals damping were considered in the calculation of abundances. Radiation damping parameters of lines were taken from VALD. In most cases the hydrogen pressure damping of metal lines was treated using the modern quantum mechanical calculations by Anstee & O’Mara (1995), Barklem & O’Mara (1997) and Barklem, O’Mara & Ross (1998). When using the Unsöld (1955) approximation, correction factors to the classical van der Waals damping approximation by widths ( $\Gamma_6$ ) were taken from Simmons & Blackwell (1982). For all other species a correction factor of 2.5 was applied to the classical  $\Gamma_6$  ( $\Delta \log C_6 = +1.0$ ), following Mäcke et al. (1975). For lines stronger than  $100 \text{ m\AA}$  the correction factors were selected individually by inspection of the solar spectrum.

Stellar rotation was taken into account when it had noticeable influence to the profiles of lines. For HD 26076, HD 28191, HD 38645, HD 50371, and HD 83805 the values of  $v \sin i$  were taken from De Medeiros & Mayor (1999); for the star HD 225216 from Hekker & Meléndez (2007); for HD 5772 from Jones et al. (2011); and for HD 35062, HD 83805, HD 223170, and HD 224533 the values of  $v \sin i$  were adjusted based on the observed spectra in this work ( $1 \text{ km s}^{-1}$  for HD 35062, and  $2 \text{ km s}^{-1}$  for the remaining three stars).

Determinations of stellar masses were performed using effective temperatures, luminosities and isochrones of Girardi et al. (2000). The luminosities were calculated from *Hipparcos* parallaxes (van Leeuwen 2007),  $V$  magnitudes were taken from SIMBAD, bolometric corrections calculated according to Alonso et al. (1999) and interstellar reddening corrections calculated using the Hakkila et al. (1994) software.

## 2.1 Estimation of uncertainties

An approximate estimate of uncertainties due to random errors of the analysis can be evaluated from the line-to-line abundance scatter which is available for the Fe I, Fe II and nitrogen abundance determinations. The mean scatter of abundances is equal to 0.04 dex.

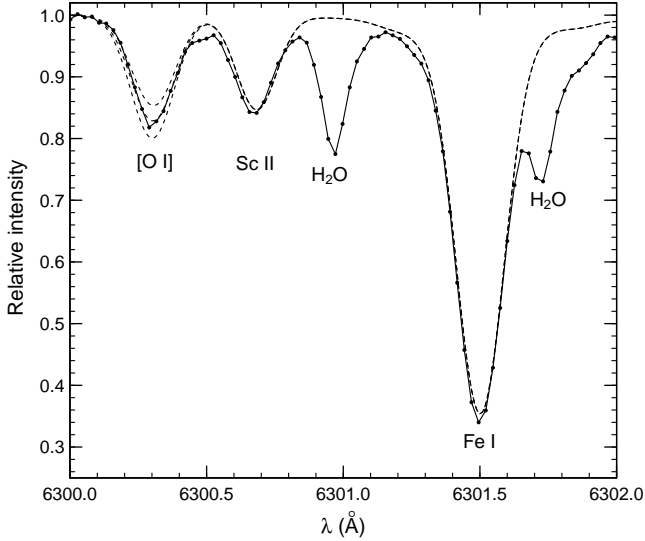


**Figure 5.** Stellar spectrum example in the region of [O I] line  $\lambda 6300.3$  Å for HD 223170 (solid line) and the synthetic spectra calculated with  $[\text{O}/\text{Fe}] = -0.13, -0.23,$  and  $-0.33$  (dashed lines).

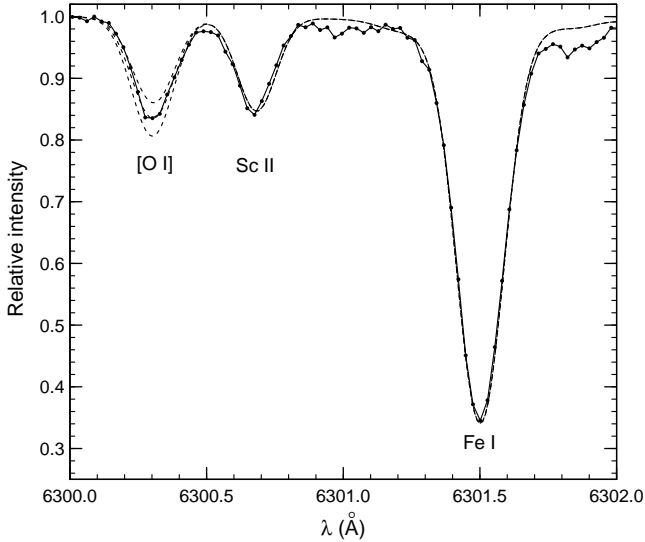


**Figure 6.** Stellar spectrum example in the region of [O I] line  $\lambda 6300.3$  Å for HD 225216 (solid line) and the synthetic spectra calculated with  $[\text{O}/\text{Fe}] = 0.06, -0.04,$  and  $-0.14$  (dashed lines).

The sensitivity of the abundance estimates to changes in the atmospheric parameters by the assumed errors is presented for the stars HD 6 and HD 55730 in Table 1.

Since abundances of C, N and O are bound together by the molecular equilibrium in the stellar atmosphere, we have also investigated how an error in one of them typically affects the abundance determination of another. In case of HD 6:  $\Delta[\text{O}/\text{H}] = 0.10$  causes  $\Delta[\text{C}/\text{H}] = 0.03$  and  $\Delta[\text{N}/\text{H}] = 0.10$ ;  $\Delta[\text{C}/\text{H}] = 0.10$  causes  $\Delta[\text{N}/\text{H}] = -0.13$  and  $\Delta[\text{O}/\text{H}] = 0.03$ .  $\Delta[\text{N}/\text{H}] = 0.10$  has no effect on either the carbon or the oxygen abundances. In case of HD 55730:  $\Delta[\text{O}/\text{H}] = 0.10$  causes  $\Delta[\text{C}/\text{H}] = 0.03$  and  $\Delta[\text{N}/\text{H}] = 0.06$ ;  $\Delta[\text{C}/\text{H}] = 0.10$  causes  $\Delta[\text{N}/\text{H}] = -0.11$  and  $\Delta[\text{O}/\text{H}] = 0.02$ .  $\Delta[\text{N}/\text{H}] = 0.10$  has no effect on either the carbon or the oxygen abundances.

**Table 1.** Effects on derived abundances resulting from model changes. The table entries show the effects on the logarithmic abundances relative to hydrogen,  $\Delta[\text{A}/\text{H}]$

Star	Species	$\Delta T_{\text{eff}}$ +100 K	$\Delta \log g$ +0.3	$\Delta v_t$ +0.3 km s <sup>-1</sup>
HD 6	C (C <sub>2</sub> )	0.01	0.03	0.00
	N (CN)	0.06	0.01	0.00
	O ([O I])	-0.01	-0.05	-0.01
	C/N	-0.19	-0.17	0.00
	<sup>12</sup> C/ <sup>13</sup> C	0	-2	-2
HD 55730	C (C <sub>2</sub> )	0.02	0.03	0.00
	N (CN)	0.10	0.01	0.00
	O ([O I])	0.01	-0.05	-0.01
	C/N	-0.26	-0.10	0.00
	<sup>12</sup> C/ <sup>13</sup> C	+2	0	0

### 3 RESULTS AND DISCUSSION

The atmospheric parameters, abundances relative to hydrogen  $[\text{E}/\text{H}]$ , stellar masses and evolutionary stages determined for the programme stars are listed in Table 2. The evolutionary status to a star was attributed from its position on stellar evolutionary sequences in the luminosity versus effective temperature diagram by Girardi et al. (2000). HD 39099 is marked by an asterisk since is a first ascent giant which has already past the luminosity bump of giant branch and though its <sup>12</sup>C/<sup>13</sup>C isotope ratio is already lowered by extra-mixing.

Our sample of investigated stars almost does not overlap with samples of clump stars investigated in other recent studies. Only one star is in common with the sample by Mishenina et al. (2006), one with Liu et al. (2007), and 8 stars are in common with Luck & Heiter (2007). As well as in the comparison which we have made between our paper Puzeras et al. (2010) and Luck & Heiter (then we had 16 common stars), we do not find obvious systematic differences between the main atmospheric parameters determined in these studies. Luck & Heiter have provided spectroscopic and physical atmospheric parameters. When compared to the physical parameters,  $[\text{Fe}/\text{H}]_{\text{Our}} - [\text{Fe}/\text{H}]_{\text{LH}} = +0.08 \pm 0.06$  (24 stars),  $T_{\text{eff(Our)}} - T_{\text{eff(LH)}} = -1 \pm 66$ , and  $\log g_{\text{Our}} - \log g_{\text{LH}} = -0.15 \pm 0.15$ . In case of spectroscopic parameters,  $[\text{Fe}/\text{H}]_{\text{Our}} - [\text{Fe}/\text{H}]_{\text{LH}} = 0.00 \pm 0.06$ ,  $T_{\text{eff(Our)}} - T_{\text{eff(LH)}} = -88 \pm 60$ , and  $\log g_{\text{Our}} - \log g_{\text{LH}} = -0.44 \pm 0.25$ . See Puzeras et al. (2010) for a discussion and comparisons between other studies.

C, N and O abundances in the investigated stars are similar to the results of Paper I and confirm the conclusion of Paper I that compared with the Sun and dwarf stars of the Galactic disk, the mean abundance of carbon in clump stars is depleted by about 0.2 dex, nitrogen is enhanced by 0.2 dex and oxygen is close to abundances in dwarfs.

#### 3.1 Comparisons with theoretical models of extra-mixing

The determined <sup>12</sup>C/<sup>13</sup>C and C/N ratios were compared with two theoretical models.

**Table 2.** Atmospheric parameters and chemical element abundances of the programme stars

HD	$T_{\text{eff}}$ K	$\log g$	$v_t$ km s <sup>-1</sup>	[Fe/H]	$\sigma_{\text{FeI}}$	$\sigma_{\text{FeII}}$	[C/H]	[O/H]	[N/H]	$\sigma$	C/N	<sup>12</sup> C/ <sup>13</sup> C	Mass $M_{\odot}$	Ev.
6	4690	1.8	1.2	-0.03	0.03	0.05	-0.26	-0.19	0.14	0.05	1.41	19	1.4	c
417	4910	2.5	1.2	-0.13	0.03	0.03	-0.36	-0.07	0.12	0.05	1.32	9	1.6	c
448	4900	2.6	1.2	0.17	0.04	0.04	-0.10	0.18	0.47	0.08	1.07	14	2.0	c
756	4800	2.1	1.15	-0.18	0.04	0.03	-0.47	-0.29	-0.03	0.06	1.45	13	1.5	c
5722	4900	2.2	1.1	-0.19	0.03	0.03	-0.51	-0.21	0.06	0.11	1.07	10	1.5	c
9057	4870	2.3	1.3	0.02	0.04	0.03	-0.19	-0.08	0.33	0.06	1.20	19	2.5	g
18690	4680	2.2	1.2	0.10	0.04	0.05	-0.13	-0.02	0.35	0.10	1.32	15	1.8	c
21530	4630	2.1	1.1	0.17	0.04	0.04	-0.16	-0.04	0.31	0.04	1.35	18	1.4	c
26162	4750	2.5	1.2	0.12	0.05	0.04	-0.07	0.10	0.45	0.06	1.20	18	1.9	c
26076	4810	2.1	1.2	-0.06	0.03	0.05	-0.39	-0.18	0.12	0.06	1.23	11	1.9	c
28191	4660	2.1	1.2	0.07	0.04	0.07	-0.21	-0.13	0.32	0.04	1.17	24	1.6	g
28625	4870	2.5	1.2	0.07	0.04	0.03	-0.21	-0.01	0.42	0.06	0.93	24	2.4	g
31757	4740	2.0	1.1	0.17	0.03	0.04	-0.19	-0.09	0.32	0.07	1.23	22	2.6	g
35062	4950	2.3	1.2	0.17	0.03	0.04	-0.23	-0.08	0.43	0.05	0.87	24	2.6	g
39099	4650	2.2	1.2	-0.52	0.03	0.04	-	-	-	-	-	9	1.1	g*
38645	4910	2.0	1.1	-0.06	0.03	0.05	-0.42	-0.35	0.15	0.07	1.07	18	1.6	c
40460	4830	2.2	1.1	-0.13	0.03	0.05	-0.32	-0.11	0.06	0.03	1.66	-	1.6	c
41125	4930	2.4	1.1	-0.07	0.04	0.05	-0.39	-0.15	0.10	0.05	1.29	24	2.2	g
41783	4820	2.0	1.1	-0.15	0.02	0.05	-0.58	-0.37	0.03	0.03	0.98	16	1.5	c
43043	4860	2.1	1.45	-0.30	0.02	0.05	-0.64	-0.36	-0.06	0.04	1.05	19	1.4	c
44061	4760	2.5	1.2	-0.18	0.03	0.04	-0.35	0.00	0.21	0.05	1.10	24	1.9	g
50371	4980	2.5	1.2	0.06	0.03	0.04	-	-	-	-	-	15	2.3	c
55730	4830	2.1	1.2	-0.14	0.03	0.06	-0.43	-0.26	0.07	0.04	1.26	10	1.4	c
63410	4860	2.0	1.05	-0.27	0.03	0.04	-0.51	-0.32	-0.17	0.06	1.82	8	1.2	c
83805	4930	2.1	1.1	0.00	0.04	0.04	-0.37	-0.23	0.35	0.08	0.76	9	2.2	c
223170	4760	2.5	1.1	0.15	0.04	0.04	-0.08	0.17	0.37	0.03	1.41	45	2.1	g
224533	4950	2.4	1.1	0.01	0.04	0.05	-0.34	-0.16	0.24	0.07	1.05	21	2.5	g
225216	4680	2.3	1.15	-0.02	0.04	0.03	-0.25	-0.06	0.16	0.02	1.55	14	1.5	c

Evolution: g – first ascent giant, c – He-core-burning star, \* – first ascent giant above the bump.

A recent so-called thermohaline model of extra-mixing provides evolutionary trends of <sup>12</sup>C/<sup>13</sup>C and C/N ratios versus stellar masses for solar metallicity stars (Charbonnel & Lagarde 2010). In order to develop this model of mixing, the combination of new ideas and 40-yr-old predictions by Ulrich (1972) was done. Eggleton et al. (2006) found a mean molecular weight ( $\mu$ ) inversion in their  $1M_{\odot}$  stellar evolution model, occurring after the so-called luminosity bump on the red giant branch, when the H-burning shell source enters the chemically homogeneous part of the envelope. The  $\mu$  inversion is produced by the reaction  ${}^3\text{He}({}^3\text{He}, 2p){}^4\text{He}$ , as predicted by Ulrich (1972). It does not occur earlier, because the magnitude of the  $\mu$  inversion is small and negligible compared to a stabilizing  $\mu$  stratification. Charbonnel & Zahn (2007) also computed stellar models including the prescription by Ulrich (1972) and extend them to the case of a non-perfect gas for the turbulent diffusivity produced by that instability in stellar radiative zone. They found that a double diffusive instability referred to as thermohaline convection, which has been discussed long ago in the literature (Stern 1960), is important in the evolution of red giants. This mixing connects the convective envelope with the external wing of the hydrogen burning shell and induces surface abundance modifications in red giant stars (Charbonnel & Lagarde 2010). Unfortunately, this model is computed so far only for solar metallicity stars.

An other so called cool bottom processing model has been developed more than a decade ago (Boothroyd et al.

1995; Wasserburg, Boothroyd & Sackman 1995; Boothroyd & Sackman 1999, and references therein). The model by Boothroyd & Sackman (1999) includes the deep circulation mixing below the base of the standard convective envelope, and the consequent "cool bottom processing" of CNO isotopes. In this model, an extra-mixing takes material from the convective envelope, transports it down to regions hot enough for some nuclear processing in the outer wing of H-burning shell, and then transports it back up to the convective envelope. For the computations of the extra-mixing, the "conveyor-belt" circulation model was used. The temperature difference between the bottom of mixing and the bottom of the H-burning shell was considered as a free parameter, to be determined by comparison with observations. For this purpose, the authors used data of M 67 (Gilroy 1989; Gilroy & Brown 1991).

In Fig. 7, <sup>12</sup>C/<sup>13</sup>C and C/N ratios versus stellar mass for galactic red clump stars analysed in Paper I and in this work are compared with the mentioned theoretical models. The carbon isotope ratio versus stellar mass plot is much more informative than the plot of carbon-to-nitrogen ratios. In the upper part of the <sup>12</sup>C/<sup>13</sup>C ratio versus stellar mass plot, along to the first dredge-up sequences of two metallicities ( $Z = 0.02$  and  $0.007$ ) the first ascent giants are located. Carbon isotope ratios of these stars are altered according to the 1<sup>st</sup> dredge-up prediction.

Helium-core-burning stars have <sup>12</sup>C/<sup>13</sup>C ratios already lowered by extra mixing and lie in the lower part of the

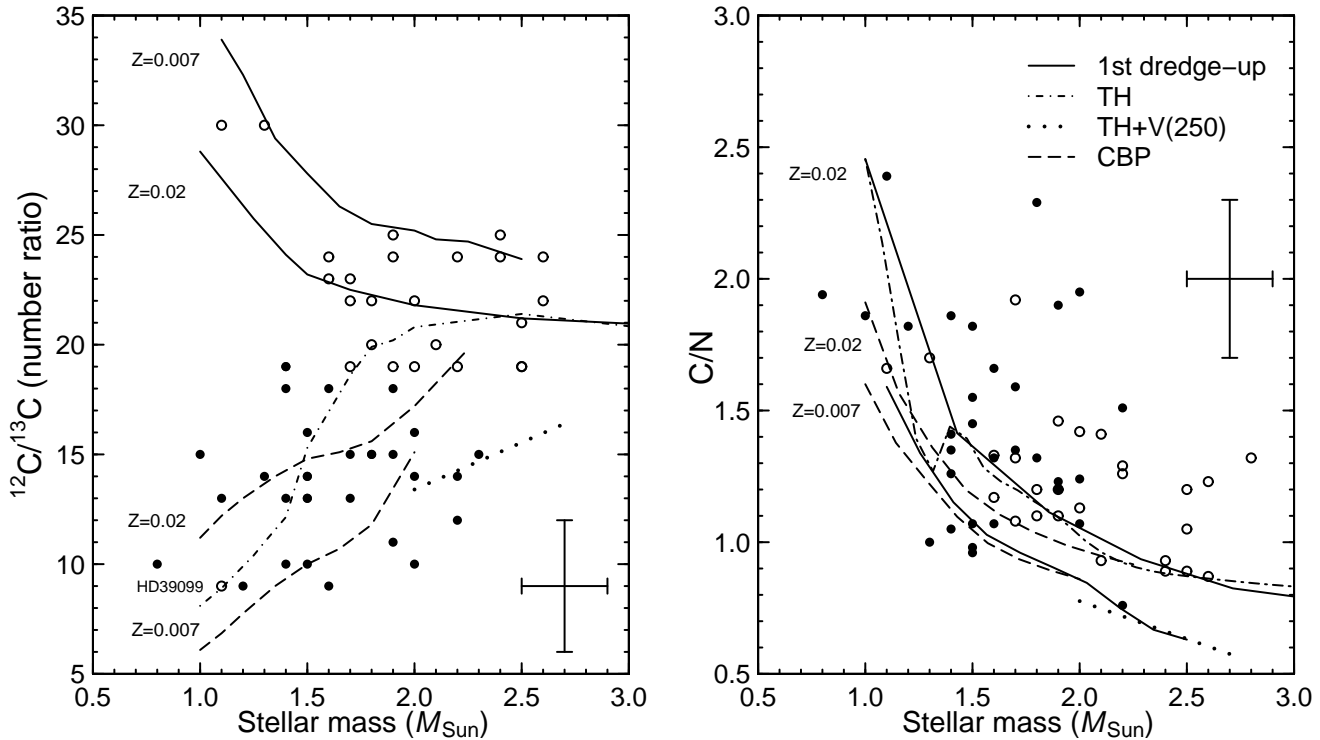


**Figure 7.**  $C/N$  and  $^{12}C/^{13}C$  ratios versus stellar turn-off mass for galactic red clump stars analysed in Paper I and this work. The stars identified as first ascent giants are shown by empty circles, and the stars identified as helium-core-burning stars – filled circles. The theoretical curves are taken from Boothroyd & Sackmann (1999) – solid and long dashed lines and Charbonnel & Lagarde (2010) – dashed-dotted and dotted lines. See Sect. 3.1 for more explanations.

$^{12}C/^{13}C$  versus stellar mass diagram. It is seen that the trend of lowering of carbon isotope ratios in low-mass He-core-burning stars is quite steep. Carbon isotope ratios may be quite different in stars of quite similar masses, for example, in stars of about  $1.5 M_{\odot}$ , the  $^{12}C/^{13}C$  values range from about 18 to 9. The theoretical model of thermohaline mixing is better reflecting the observational data in this respect than the more shallow model of cool bottom processing.

As concerns the helium-core-burning stars of higher masses, it seems that the mixing was more intense, and this might be caused by a stellar rotation while stars were in a stage of hydrogen burning in their cores. Charbonnel & Lagarde (2010) computed models with rotation-induced mixing for stars at the zero age main sequence (ZAMS) having rotational velocities of 110, 250 and  $300 \text{ km s}^{-1}$ . Typical initial ZAMS rotation velocities were chosen depending on the stellar mass based on observed rotation distributions in young open clusters (Gaige 1993). The convective envelope was supposed to rotate as a solid body through the evolution. The transport coefficients for chemicals associated to thermohaline and rotation-induced mixing were simply added in the diffusion equation and the possible interactions between the two mechanisms were not considered. Interesting to note that the rotation-induced mixing modifies the internal chemical structure of main sequence stars, although its signatures are revealed only later in the stellar evolution.

In Fig. 7 we plotted a model corresponding to the rotational velocity of  $250 \text{ km s}^{-1}$ . The observational data for stars of about  $2 M_{\odot}$  in our sample require a modelling of mixing with rotation of about this speed when stars were on the main sequence. Even large rotationally induced mixing

is suggested by stars of high masses in open clusters (e.g. Tautvaišienė et al. 2005; Smiljanic et al. 2009; Mikolaitis et al. 2010, 2011b).

### 3.2 Membership of the Galactic red clump

The stellar positions in the  $^{12}C/^{13}C$  versus stellar mass diagram as well as comparisons to stellar evolutionary sequences in the luminosity versus effective temperature diagram may show which stars are helium-core-burning ones and which are first ascent giants. From the available sample of 62 Galactic red clump stars investigated in this work and Paper I, 35 were identified as helium-core-burning ones and 27 as first ascent just hydrogen-shell-burning giants. In the paper by Mishenina et al. (2006), according to nitrogen abundance values, the authors have suggested 21 helium-core-burning stars, about 54 candidates to helium-core-burning stars and about 100 first ascent giants. Looking to the density of stars above and below the clump in the colour-magnitude diagram for the *Hipparcos* catalogue, it seems that a number of helium-core-burning stars in the Galactic red clump should be slightly larger than a number of first ascent giants. For example, if we count a number of stars in a frame of  $M_v = 2 \pm 0.5$  and  $0.8 < B - V < 1.2$  targeted on the clump, we count 1050 stars, while below the clump, in a frame of  $M_v = 1 \pm 0.5$  and  $0.8 < B - V < 1.2$ , we have 380 stars.

A very promising way to distinguish between hydrogen- and helium-burning red giant stars was recently uncovered by asteroseismic observations (Bedding et al. 2011). From high-precision photometry obtained by the KEPLER space

observatory, it was found that gravity-mode period spacings are different in hydrogen- and helium-burning red giants. In hydrogen-shell-burning stars the period spacing is mostly about 50 seconds, and in helium-burning stars it is from about 100 to 300 seconds. These differences appear because of differences of internal structure and core densities of stars. This asteroseismic way of stellar evolutionary status determination is especially important for stars of larger than  $2 M_{\odot}$  masses for which chemical composition signatures of extra-mixing are less trustful.

### 3.3 Conclusions

In this work we present the main atmospheric parameters, abundances of nitrogen, carbon and oxygen, and  $^{12}\text{C}/^{13}\text{C}$  ratios for a sample of 28 Galactic clump stars from high-resolution spectra observed on the Nordic Optical telescope ( $R \approx 80\,000$ ).

The mean abundances of C, N and O in the investigated clump stars support our previous estimations (Paper I) that compared to dwarf stars of the Galactic disk carbon is depleted by about 0.2 dex, nitrogen is enhanced by 0.2 dex and oxygen is close to abundances in dwarfs.

The  $^{12}\text{C}/^{13}\text{C}$  and C/N ratios for the galactic red clump stars analysed were compared to the evolutionary models of extra-mixing. The steeper drop of  $^{12}\text{C}/^{13}\text{C}$  ratio in the model of thermohaline mixing (Charbonnel & Lagarde 2010) better reflects the observational data at low stellar masses than the more shallow model of cool bottom processing (Boothroyd & Sackman 1999).

In our sample, for stars of about  $2 M_{\odot}$  masses the modelling of rotationally induced mixing should be considered with rotation of about  $250 \text{ km s}^{-1}$  at the time when a star was at the hydrogen-core-burning stage.

The stellar positions in the  $^{12}\text{C}/^{13}\text{C}$  versus stellar mass diagram as well as comparisons to stellar evolutionary sequences in the luminosity versus effective temperature diagram by Girardi et al. (2000) show that from the investigated sample of Galactic red clump stars about a half are first ascent giants with carbon isotope ratios altered according to the first dredge-up prediction, and an other half are helium-core-burning stars with carbon isotope ratios altered by extra-mixing.

### ACKNOWLEDGEMENTS

We wish to thank sincerely B. Edvardsson, B. Gustafsson and K. Eriksson (Uppsala Observatory) for providing computing codes and atomic data for this work. This project has been supported by the European Commission through ‘‘Access to Research Infrastructures Action’’ of the ‘‘Improving Human Potential Programme’’, awarded to the Instituto de Astrofísica de Canarias to fund European Astronomers’ access to the European Northern Observatory, in the Canary Islands.

### REFERENCES

Alonso A., Arribas S., Martínez-Roger C., 1999, *A&AS*, 140, 261

Angelou G. C., Stancliffe R. J., Church R. P., Lattanzio J. C., & Smith G. H. 2012, *ApJ*, 749, 128  
 Anstee S. D., & O’Mara B. J., 1995, *MNRAS*, 276, 859  
 Barklem P. S., & O’Mara B. J., 1997, *MNRAS*, 290, 102  
 Barklem P. S., O’Mara B. J. & Ross J. E., 1998, *MNRAS*, 296, 1057  
 Bedding T. R. et al. 2011, *Nat*, 471, 608  
 Boothroyd A. I., Sackmann I.-J., 1999, *ApJ*, 510, 232  
 Cantiello M., Langer N. 2010, *A&A*, 521, 9  
 Chanamé J., Pinsonneault M., Terndrup D., 2005, *ApJ*, 631, 540  
 Charbonnel C. 1994, *A&A*, 282, 811  
 Charbonnel C., Brown J. A., & Wallerstein G. 1998, *A&A*, 332, 204  
 Charbonnel C., 2006, in Montmerle T., Kahane C., eds., *Stars and Nuclei: Tribute to Manuel Forestini*, EAS Publ. Ser., vol. 19, 125  
 Charbonnel C., Zahn J.-P., 2007, *A&A*, 467, L15  
 Charbonnel C., & Lagarde N. 2010, *A&A*, 522, A10  
 Day R. W., Lambert D. L., Sneden C., 1973, *ApJ*, 185, 213  
 De Medeiros J. R., Mayor M., 1999, *A&AS*, 139, 433  
 Denissenkov P. A. 2010, *ApJ*, 723, 563  
 Eggleton P. P., Dearborn D. S. P., & Lattanzio J. C. 2006, *Sci*, 314, 1580  
 Gaige Y. 1993, *A&A*, 269, 267  
 Gilroy K. K. 1989, *ApJ*, 347, 835  
 Gilroy K. K., & Brown J. A. 1991, *ApJ*, 371, 578  
 Girardi L., Bressan A., Bertelli G., Chiosi C., 2000, *A&AS*, 141, 371  
 Gratton R. G., Sneden C., Carretta E., Bragaglia A., 2000, *A&A*, 354, 169  
 Gratton R., Bragaglia A., Carretta E., Tosi M., 2006, *ApJ*, 642, 462  
 Grevesse N., Sauval A. J., 2000, in Manuel O., ed., *Origin of Elements in the Solar System, Implications of Post-1957 Observations*, (Kluwer), p. 261  
 Gurtovenko E. A., & Kostik R. I., 1989, *Fraunhofer’s spectrum and a system of solar oscillator strengths*, Kiev, Naukova Dumka, 200 p.  
 Gratton R., Bragaglia A., Carretta E., Tosi, M., 2006, *ApJ*, 642, 462  
 Gustafsson B., Edvardsson B., Eriksson K., Jørgensen U. G., Nordlund Å., Plez B., 2008, *A&A*, 486, 951  
 Hakkila J., Myers J. M., Stidham B.J., Hartmann D. H., 1994, *AJ*, 114, 2043  
 Hekker S., Meléndez J., 2007, *A&A*, 475, 1003  
 Iben I., 1965, *ApJ*, 142, 1447  
 Ilyin I. V., 2000, *High resolution SOFIN CCD échelle spectroscopy*, PhD dissertation, Univ. Oulu, Finland  
 Johansson S., Litzén U., Lundberg H., Zhang Z., 2003, *ApJ*, 584, 107  
 Jones M. I., Jenkins J. S., Rojo P., Melo C. H. F., 2011, *A&A*, 536, 71  
 Kurucz R. L., 2005, *Mem. Soc. Astron. Ital. Suppl.* 8, 189  
 Solar Observatory, Sunspot, New Mexico  
 Lagarde N., Charbonnel C., Decressi, T., & Hagelberg J. 2011, *A&A*, 536, A28  
 Lambert D. L., Ries L. M. 1977, *ApJ*, 217, 508  
 Lambert D. L., Ries L. M., 1981, *ApJ*, 248, 228  
 Liu Y. J., Zhao G., Shi J. R., Pietrzynski G., Gieren W., 2007, *MNRAS*, 382, 553  
 Luck R. E., Heiter U., 2007, *AJ*, 133, 2464

- Mäckle R., Holweger H., Griffin R., Griffin R., 1975, *A&A*, 38, 239
- Mikolaitis Š., Tautvaišienė G., Gratton R., Bragaglia A., & Carretta E. 2010, *MNRAS*, 407, 1866
- Mikolaitis Š., Tautvaišienė G., Gratton R., Bragaglia A., & Carretta E. 2011a, *MNRAS*, 413, 2199
- Mikolaitis Š., Tautvaišienė G., Gratton R., Bragaglia A., & Carretta E. 2011b, *MNRAS*, 416, 1092
- Mikolaitis Š., Tautvaišienė G., Gratton R., Bragaglia A., & Carretta E. 2012, *A&A*, 541, 137
- Mishenina T. V., Bienaymé O., Gorbaneva T. I., Charbonnel C., Soubiran C., Korotin S. A., Kovtyukh V. V., 2006, *A&A*, 456, 1109
- Pagel B. E. J., 1974, *MNRAS*, 167, 413
- Palmerini S., La Cognata M., Cristallo S., & Busso, M. 2011, *ApJ*, 729, 3
- Perryman M.A.C. et al., 1997, *A&A*, 323, L49
- Piskunov N. E., Kupka F., Ryabchikova T. A., Weiss W. W., & Jeffery C. S., 1995, *A&AS* 112, 525
- Puzeras E., Tautvaišienė G., Cohen J. G., Gray D. F., Adelman S. J., Ilyin I., Chorniy Y., 2010, *MNRAS*, 409, 1213
- Recio-Blanco A., de Laverny P., 2007, *A&A*, 461, L13
- Simmons G.J., & Blackwell D.E., 1982, *A&A* 112, 209
- Smiljanic R., Gauderon R., North P., Barbuy B., Charbonnel C., Mowlavi N., 2009, *A&A*, 502, 267
- Spite M. et al., 2006, *A&A*, 455, 291
- Stern M. E., 1960, *Tellus*, 12, 172
- Tautvaišienė G., Edvardsson B., Tuominen I., Ilyin I., 2000, *A&A*, 360, 499
- Tautvaišienė G., Edvardsson B., Tuominen I., Ilyin I., 2001, *A&A*, 380, 578
- Tautvaišienė G., Puzeras E., Gray D. F., Ilyin I., 2003, in Piskunov N. E., Weiss W. W. & Gray D. F., eds., *Proc. IAU Symp. 210, Modelling of Stellar Atmospheres*, Published on behalf of the IAU by the Astronomical Society of the Pacific, p. D6
- Tautvaišienė G., Edvardsson B., Puzeras E., Ilyin I., 2005, *A&A*, 431, 933
- Tautvaišienė G., Edvardsson B., Puzeras E., Ilyin I., 2007, in Kupka F., Roxburg I. W. & Chan K. L., eds., *Proc. IAU Symp. 239, Convection in Astrophysics*, p.301
- Tautvaišienė G., Puzeras E., 2009, in Andersen J., Bland-Hawthorn J., Nordström B., eds., *Proc. IAU Symp. 254, The Galaxy Disk in Cosmological Context*, p. 75
- Tautvaišienė G., Edvardsson B., Puzeras E., Barisevičius G., & Ilyin I. 2010, *MNRAS*, 409, 1213 (Paper I)
- Tomkin J., Luck R. E., Lambert D. L., 1976, *ApJ*, 210, 694
- Tuominen I., Ilyin I., Petrov P., 1999, in Karttunen H., Piironen V., eds., *Astrophysics with the NOT*, Turku University, Piikio, Finland, p. 47
- Ulrich R. K., 1972, *ApJ*, 172, 165
- Unsöld A., 1955, *Physik der Stern Atmosphären (Zweite Auflage)*. Springer-Verlag, Berlin
- van Leeuwen F. 2007, *Astrophysics and Space Science Library*, Vol. 350
- Wachlin F. C., Miller Bertolami M. M., & Althaus L. G. 2011, *A&A*, 533, A139
- Wasserburg G. J., Boothroyd A. I., & Sackmann I.-J. 1995, *ApJL*, 447, L37

This paper has been typeset from a  $\text{\TeX}$ / $\text{\LaTeX}$  file prepared by the author.